

SPECTRAL STUDIES OF A SELENIUM(IV) VITAMIN B3 COMPOUNDS PREPARED IN THE FORM OF NANOMETER USING SIMPLE CHEMICAL REACTIONS TO FURTHER USE AS ANTIOXIDANT IN THE PREPARATION OF DRUGS

Mohamed Y. El-Sayed^{1*}, Ibrahim M.A. Alatawy¹, Hazim M. Ali¹, A. Muqbil Alsirhani¹, Yasser A. El-Ossaily¹, Khaled Shalaby² and Moamen S. Refat³

¹Department of Chemistry, College of Science, Jouf University, Sakaka 2014, Saudi Arabia

²Department of Pharmaceutics, College of Pharmacy, Jouf University, Sakaka P.O. Box 2014, Saudi Arabia

³Department of Chemistry, College of Science, Taif University, P.O. Box 11099, Taif 21944, Saudi Arabia

(Received June 28, 2024; Revised July 30, 2024; Accepted August 1, 2024)

ABSTRACT. The current study dealt with selenium metal ion complexes with mixed ligands, consisting of nicotinamide (vitamin B3) as the first ligand, and amino acids such as (histidine, tryptophan, and tyrosine) as the second ligand. It was synthesized in (1:1:1) (selenium: vitamin: amino acid) in molar ratio. By using different characterization techniques such as elemental analysis, the conductance, FTIR, XRD, UV-Vis, TG/DTG, ¹H-NMR, XRD, SEM, TEM analyses, the chemical structures and the morphological properties of the synthesized complexes were checked and discussed. The nicotinamide was coordinated as monodentate ligand *via* the nitrogen of pyridine ring but all amino acids as a secondary ligand coordinated as bidentate through oxygen of carboxylic group and nitrogen of amino group. The complexes demonstrate antioxidant activity with potent scavenging property, the synthesized in the form of nanometer give great importance in increasing efficiency of absorption of human cells to selenium giving the highest efficiency of medical product. All complexes in this study were evaluated for their anticancer effect towards HepG2 and A2780 cell lines. From these data the complex (Se/Nia/ Tyr) can be used as antitumor agents.

KEY WORDS: Selenium, Amino acids, Vitamin B3, Mixed ligand, Complexes, Antioxidant

INTRODUCTION

Selenium is one of the trace elements which plays an active role in many biological systems [1] and has great importance in nutrition and medicine [2, 3]. Selenium similarly to Sulfur owing to present in the same group it's have tendency to form compounds involved in biological systems [4] and both have ability to transfer light to electricity which is called photovoltaic and photoconductive, which has important use in photography, solar cells, and xerography. Selenium exists in one of three biological forms in the body. First one, selenoproteins which consists of selenocysteine residues and play essential selenium-dependent roles in oxidation and reduction reactions. Second, selenium binds with nonspecific plasma proteins such as albumin, globulins and may help in distribution of selenium; they may directly bond selenium or contain it as selenocysteine or selenomethionine instead of cysteine and methionine, respectively. Third, there are many forms inorganic of inorganic selenium in transport throughout the body, such as selenate, selenides, and selenium (Se⁰) element. The known specific selenoproteins-glutathione peroxidase, iodothyronine5-deiodinases, and thioredoxin reductase at the active site contain a selenocysteine residue. The most research of these is glutathione peroxidase, which corresponds to detoxification of reactive species of oxygen [5, 6]. The deficiency of Selenium affects about half a billion person each year [7] A lot of diseases may develop and worsen, such as, depression [8], cardiovascular crises, tumor disorders, thyroid dysfunction, or spread of viruses [9], it is

*Corresponding authors. E-mail: myelsayed@ju.edu.sa

This work is licensed under the Creative Commons Attribution 4.0 International License

lowering the viability of sperms [10], but some studies also published about the selenium's ability of delaying ageing [11, 12].

Recently amino acids have attracted a lot of interest as effective chelators because they form strong chemical bonds [13]. The mineral atoms that function as food minerals are those that are of interest [14]. Twenty natural amino acids make up the basic components of proteins and are necessary for the execution of a wide range of biological processes [15]. The coordination statement occurs naturally in the body to facilitate the transfer of minerals across the intestinal wall as part of digestion process [16]. The complexity of mineral amino acids in recent years are useful as antitumor agents, and antimicrobial agents. Amino acid's structure containing two main groups (carboxylic acid and amine) which attached to chiral carbon atoms are significant in the study of biochemistry. α -Amino acid general chemical formula is $H_2NCHR\text{COOH}$ [17]. Amino acids are the fundamental chemical components of proteins, which take part in the formation of all living things and play a vital role in biochemical processes [18]. Their chelating group NH_2 or $COOH$ groups allow them to coordinate excellent with transition metals, making them very capable of being great catalysts [19]. It was discovered that protein structural stability and enzymatic activity are both caused by interactions involving amino acids [20]. A useful area of research is the complexity of mineral amino acids, which can be used in computer simulations to identify the interaction of metalloprotein in biological systems. [21-26].

With the ability to achieve an increased therapeutic impact while combining with a decreased toxicity, the research field of metal drug complexes has recently attracted significant interest. We are aware of very little research on the chelation of vitamin A with selenium(IV) metal ions, and the literature has no interpretation explanation for spectroscopic characterizations. The explanation is dependent on the drug capacity to form complex relate with vital metal ions antioxidant like selenium(IV). The vitamin B_{13} known as orotic acid (OA), which assists with vitamin B_9 metabolism, is a nucleic acid base, particularly the uracil base, acts as an intermediate in the production of pyrimidines [27]. This substance is employed in medicine as a bio-stimulator of ionic exchange mechanisms [28-36]. The focus of the current work was on synthesized new selenium(IV) complexes with mixed ligands, which included histidine, tryptophan, and tyrosine as the second ligand and one of an interesting vitamins like vitamin B_3 , as the first ligand.

EXPERIMENTAL

Chemicals

All chemicals in this study were used without any further treatment. Distilled water used in all the experiments was obtained by Milli-Q direct 8 purification system (Millipore, France). Amino acids Tyr, Trp, His, nicotinamide (Nia), and $SeCl_4$ were purchased from (Sigma-Aldrich). NH_4OH , methanol, diethyl ether, dimethyl sulfoxide (sigma, Aldrich).

Synthesis of Se amino acid-nicotinamide mixed ligand complexes

The complexes were prepared with stoichiometry $Se:L_1:L_2$ (1:1:1) where $L_1 = His, Trp, Tyr$ and $L_2 = nicotinamide$. A mixture of 25 mL (1 mmol) of methanol solution of amino acid and 25 mL (1 mmol) of methanol solution of nicotinamide were added slowly to 25 mL (1 mmol) of $SeCl_4$ in methanol solution. After neutralization using ammonium hydroxide, the solution was refluxed for 4 hours at 60 °C. The resulting faint brown to red-brown solution was reduced to half of their volume then the solid precipitate was collected and washed with hot methanol and dried over anhydrous $CaCl_2$.

Instrumentations

The molar conductance of the prepared 10 mol/cm³ Se(IV) complexes in DMSO solution was measured by HANNA Edge conductivity meter. The microanalytical analyses (% carbon, % hydrogen and % nitrogen) contents have been measured by using a Perkin Elmer CHN 2400 (USA). The metal content was determined gravimetrically by converting the compounds into their corresponding carbides or oxides. IR spectroscopy is used to characterize a new substance. First, a background spectrum is performed to provide a relative scale for transmittance strength, the yield spectrum in which the instruments attributes are disregarded, such that the spectra produced from samples contain just the spectral features of the samples. FT-IR spectra is considered molecular fingerprint of the material. Infrared spectra of Se(IV) complexes were measured in the range of 400-4000 cm⁻¹ on FT-IR Nicolet 6700, Thermo scientific, USA. The ¹H-NMR spectra of Se complexes were recorded on JEOL resonance NMR spectrometer, using DMSO-d₆ as solvent and TMS as an internal reference. Thermogravimetric analysis was carried out in the temperature range of 25 to 600 °C in nitrogen atmosphere by thermogravimetric analyzer, Shimadzu, TGA-51 with heating rate 10 °C/min with platinum crucible X-ray diffractometer (Bruker D8 Adv., Germany) with Ni-filtered Cu-Kα line as the radiation source (λ = 1.54056 Å) was used to create XRD patterns. X-ray diffractogram rang in 2θ = 10-80° at room temperature. The UV-Vis spectra were measured in DMSO solvent with concentration (10⁻³ M) for the free amino acids, vitamins ligands and their complexes using Agilent Cary 60 spectrophotometers (Agilent technologies, USA) with 1 cm quartz cell, in the range 200-900 nm. Scanning electron microscopy was used to analyze the morphological of the surface using (SEM, JEOL.JSM-6610LV, Tokyo, Japan) SEM employs a scan of closely focused electron beam across the surface of the samples. The transmission electron microscopy images were performed using JEOL JEM-1200 EX II, Japan at 60-70 kV.

Antioxidant activities Assessment

The scavenging activity of all produced compounds was assessed against DPPH (diphenyl picryl hydrazyl) [37]. The stable free radical DPPH can convert into a stable, diamagnetic molecule by accepting an electron or a hydrogen radical. At 517 nm, DPPH has a significant absorption band. To reach a critical concentration (0.1 mmol/L), the test samples were dissolved in 1.5 mL of aqueous methanol (0.2 mmol/L) and then added to an equivalent volume of (0.2 mmol/L) DPPH solution. Several test solution concentrations (2.5, 5, and 10 µg/mL) were added to the DPPH solution. The absorbance was measured at 517 nm against a blank after 30 min of incubation at 20 °C with vigorous shaking. The experiment was run three times, and the outcomes were averaged. Equation 1 was used to calculate the % of inhibition (I%) of free radical generation from DPPH.

$$\% I = \frac{A_{control} - A_{sample}}{A_{control}} \times 100 \quad (1)$$

where after t = 30 min A sample is the absorbance of various absorptions and A control is the absorbance of a blank DPPH serves as a check (alone).

Cytotoxicity and anticancer activity

The cytotoxicity of medications is evaluated using the colorimetric MTT test. The determine cell viability, the MTT test involves the reduction of MTT, a tetrazolium dye, to insoluble formazan (purple color) in living cells [38] By adding an appropriate solvent, the insoluble purple formazan is converted into a colorful solution. This colored solution's absorbance can be measured at a specific wavelength of 570 nm. By comparing the amount of purple formazan produced by

untreated control cells with dosage response curves, it is possible to estimate a drug's capacity to kill cells. (100 μL per well) in a 96-well plate was used to seed the cancer cells. Cells were cultured with 50 μM of each test substance or DMSO (0.5% v/v) for an entire night at 37 $^{\circ}\text{C}$ and 5% CO_2 . MTT (3-(4,5-dimethylthiazoyl)-2,5-diphenyl-tetrazolium bromide (MTT) (5 mg/mL phosphate buffered saline (PBS)) was added to the plate after 48 hours of incubation, and the plate was then incubated for 4 hours. After that, formazan crystals were dissolved using an acidified sodium dodecyl sulfate (SDS) solution (10% SDS with 0.01 N HCl in 1x PBS). A Biotek plate reader (Gen5TM) was used to measure the absorbance at a wavelength of between 570 and 630 nm after 14 hours of incubation [39-42]. Based on the results of the preliminary screening, the cells were exposed to serial dilutions of compounds 1-6 for 48 hours, after which the vitality of the cells was assessed using the MTT reagent.

RESULTS AND DISCUSSION

Microanalytical and molar conductance measurements

The synthesized selenium(IV) mixed ligand complexes were isolated in solid state forms which are stable in room temperature and soluble in DMSO as organic solvent. The molar conductance values of $[\text{Se}(\text{Nia})(\text{His})\text{Cl}]\text{Cl}_2$ (I), $[\text{Se}(\text{Nia})(\text{Trp})\text{Cl}]\text{Cl}_2$ (II) and $[\text{Se}(\text{Nia})(\text{Tyr})\text{Cl}]\text{Cl}_2$ (III) are 97, 93 and 102 $\Omega^{-1}\text{cm}^2 \text{mol}^{-1}$, respectively confirmed that the electrolytic nature for the three complexes, because the presence of two chloride ions outside the coordination sphere and one chloride ion inside the coordination sphere [43]. The presence of coordinated chloride was characterized using AgNO_3 . Elemental analysis data (Table 1) % carbon, % hydrogen and % nitrogen as well as % Se metal was in good agreement with the proposed structure formula.

Table 1. Elemental analysis and physical results of $[\text{Se}(\text{Nia})(\text{AA})^{-1}]$ complexes (AA = His, Trp and Tyr).

Complexes	M.wt g/mol	Color	m.p. $^{\circ}\text{C}$	(Cal.)/Found			M.C.
				%C	%H	%N	
(I)	460.59	Faint brown	>250 $^{\circ}\text{C}$	(31.29) 30.9	(2.84) 3.8	(15.2) 14.3	97
(II)	509.67	Reddish brown	>250 $^{\circ}\text{C}$	(40.1) 39.4	(3.3) 3.9	(10.9) 11.8	93
(III)	486.63	Dark brown	>250 $^{\circ}\text{C}$	(37.02) 36.2	(3.10) 3.5	(8.63) 9.1	102

M.C. = Molar conductance, $\Omega^{-1}\text{cm}^2 \text{mol}^{-1}$.

Electronic spectra

UV-Vis spectra of Se(IV)/Nia/amino acid mixed ligand complexes in DMSO solvent are measured, showing noticeable absorption peaks within the region of 270-490 nm. The formation of nicotinamide/amino acids SeNPs was confirmed using UV-Vis electronic spectral scanning, due to change the color from colorless of Se(IV) chloride to brown – reddish brown colored (SeNPs), with absorption maximum (λ_{max}) at (270-390 nm). The charge transfer from ligand to metal $\text{M} \rightarrow \text{L}$, was allocated to absorption band at 480 nm [44].

Infrared spectral studies

The IR spectrum of $[\text{Se}(\text{Nia})(\text{AA})]$ complexes (**1-3**) are shown in Figure 1. In Table 2, the bands $\nu_{\text{as}}(\text{N-H})$ and $\nu_{\text{s}}(\text{N-H})$ of CONH_2 group are shifted to lower or higher wavenumber in comparison with free nicotinamide, it might be explained by the formation of hydrogen bonds between the NH_2 and CO group [45]. The recorded FT-IR spectra of Se nanoparticle complexes (**1-3**) did not

notice the participation of nitrogen of amido group in complexation with Se. The spectra of the complexes showed a shift in the pyridine ring bands of free nicotinamide at 1599, 1570, and 1400 cm^{-1} , indicating involvement of nitrogen atom of pyridine ring in coordination. Overall, spectra illustrate that nicotinamide was binding as a monodentate ligand. The bands of $\nu_{\text{as}}(\text{N-H})$ and $\nu_{\text{s}}(\text{N-H})$ appeared at (3360-3110 cm^{-1}) and (3120-3090 cm^{-1}), respectively in the spectra of free amino acid were shifted to higher wave number (3420-3350 cm^{-1}) and (3195-3100 cm^{-1}) in the spectra of the complex, which proposed coordinating the amino group with the metal through nitrogen. The coordination of a carboxylic acid group via oxygen with selenium was revealed by the shift of the free amino acids as $\nu_{\text{as}}\text{COO}^-$ wavenumber to a lower one in the complexes' spectra. The difference between $\nu_{\text{s}}\text{COO}^-$ and $\nu_{\text{as}}\text{COO}^-$ increased as the M-O bond character became more covalent. Therefore, in the complex neutral nicotinamide ligand coordinate via pyridine nitrogen the amino group nitrogen and carboxylate oxygen in the amino acid served as a monobasic bidentate ligand. The bands observed at the 530-590 cm^{-1} and 510-425 cm^{-1} assigned to $\nu(\text{M-O})$ and $\nu(\text{M-N})$ vibrations, respectively.

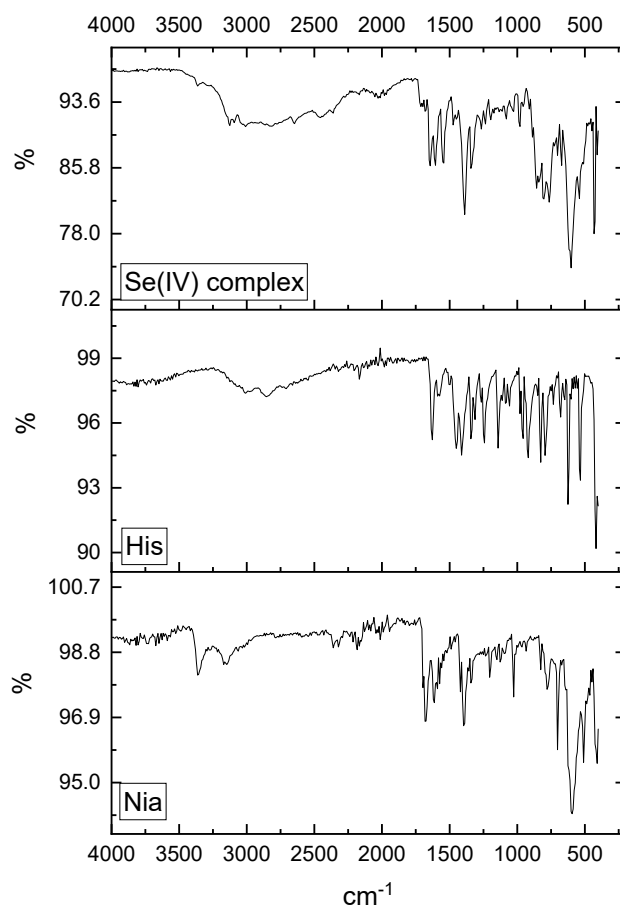


Figure 1a. Infrared spectra of nicotinamide (Nia), histidine (His) ligands and Se(IV) complex.

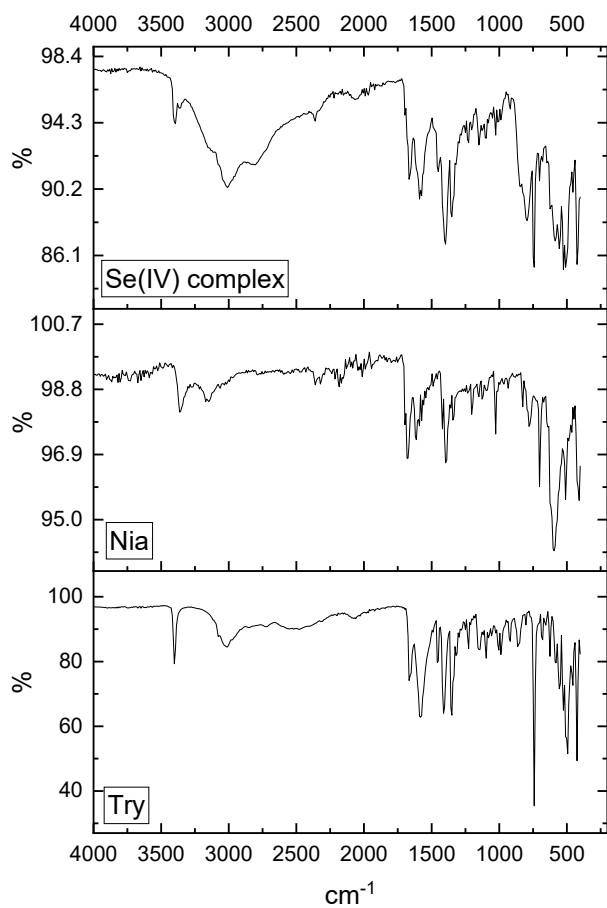


Figure 1b. Infrared spectra of nicotinamide (Nia), tryptophan (Try) ligands and Se(IV) complex.

Table 2. The IR spectral bands of $[\text{Se}(\text{Nia})(\text{AA})^{-1}]$ complexes.

Compounds	Assignments				
	$\nu_{\text{as}}(\text{NH}_2)$	$\nu_{\text{s}}(\text{NH}_2)$	$\delta(\text{NH}_2)$	$\nu_{\text{as}}(\text{COO}) + \text{Ph}$	$\nu_{\text{s}}(\text{COO})$
Nia	3370	3170	1660	1599, 1570, 1340	--
His (I)	3400, 3300	3190	1680	1615, 1410	1410
Trp (II)	3420, 3390	3200	1695	1612, 1410	1400
Tyr (III)	3200	3100	1699	1609, 1399	1399

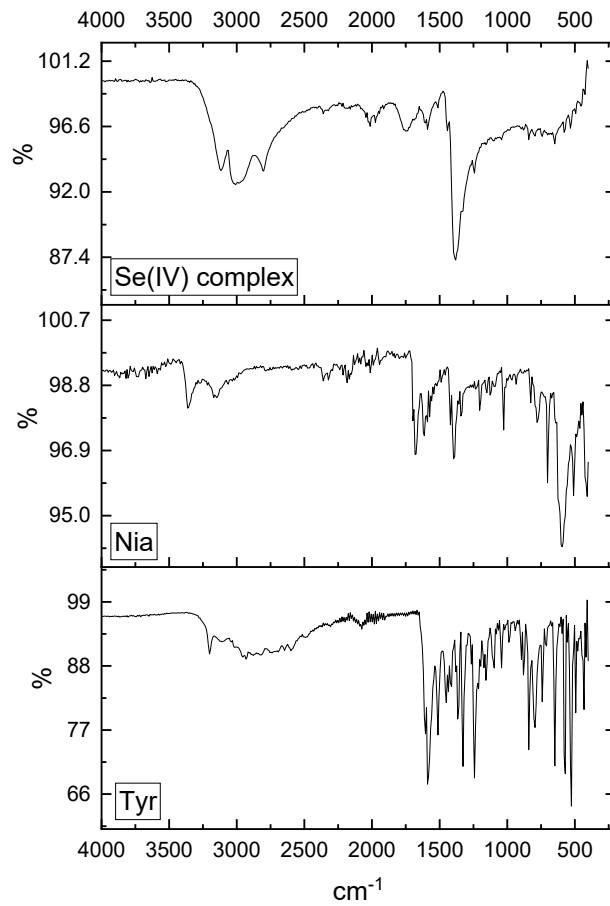
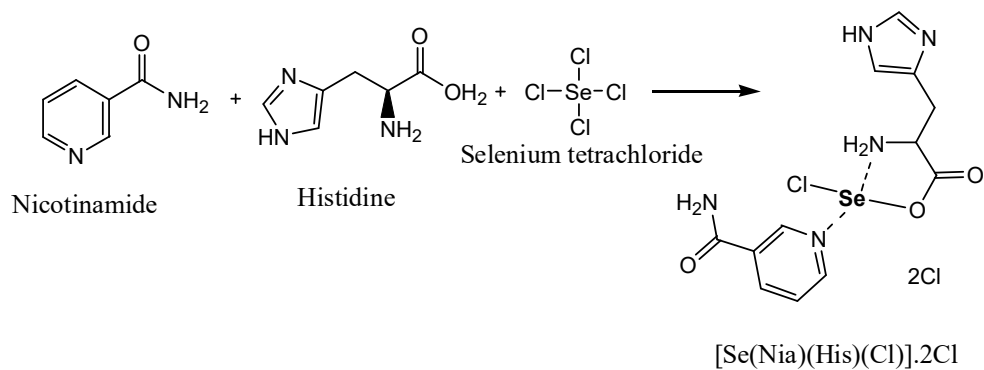


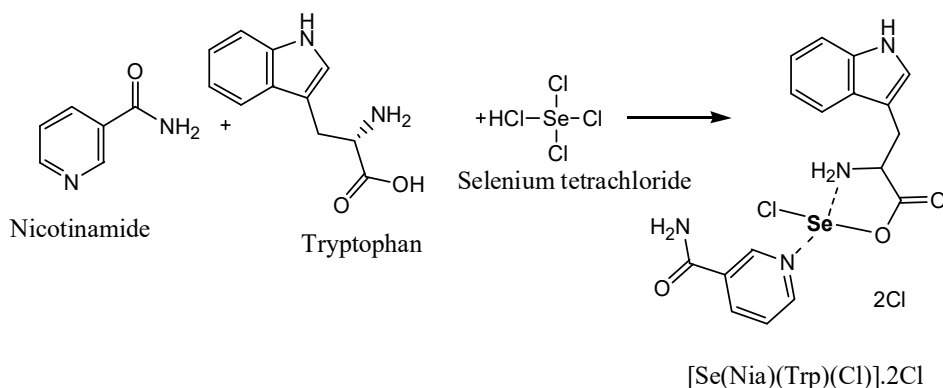
Figure 1c. Infrared spectra of nicotinamide (Nia), tyrosine (Tyr) ligands and Se(IV) complex.

¹H-NMR spectra studies



Scheme 1. The association pathway of [Se(Nia)(His)(Cl)].2Cl complex.

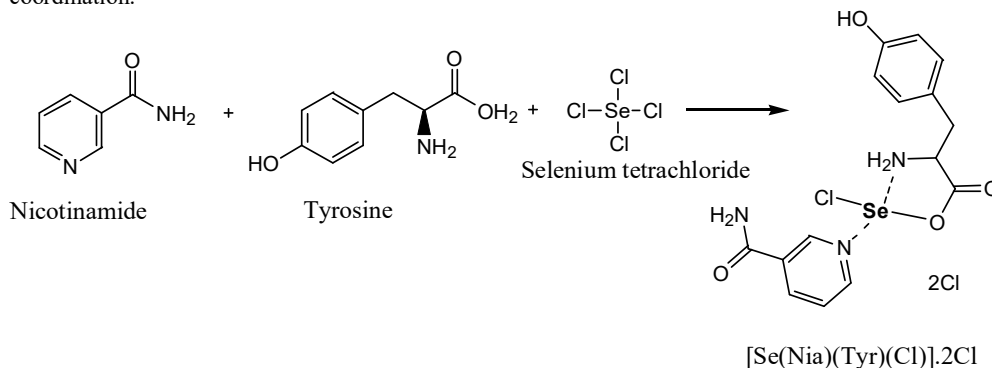
$^1\text{H-NMR}$ (DMSO-d_6) spectral data of nicotinamide $\delta = 9.00, 8.76, 8.20, 7.55$ (4H, aromatic pyridine ring), and 7.80 (2H, NH_2); $^1\text{H-NMR}$ (DMSO-d_6) spectral data of histidine $\delta = 13.00$ (1H, NH imidazole ring), 12.89 (1H, $-\text{OH}$ propanoic acid), 8.64 (2H, NH_2), $8.73, 7.66$ (2H, aromatic imidazole ring), 4.18 (1H, $-\text{CH}$ propanoic acid), and $3.17, 2.92$ (2H, $-\text{CH}_2$ propanoic acid); $^1\text{H-NMR}$ (DMSO-d_6) spectral data of $[\text{Se}(\text{Nia})(\text{His})(\text{Cl})].2\text{Cl}$ complex (Scheme 1) $\delta = 9.00, 8.70, 8.10, 7.60, 7.50, 6.10$ (protons of aromatic imidazole ring, pyridine ring and NH_2), $3.46, 2.45$ (protons of $-\text{CH}, -\text{CH}_2$ propanoic acid). The $^1\text{H NMR}$ spectrum of the $[\text{Se}(\text{Nia})(\text{His})(\text{Cl})].2\text{Cl}$ complex was recorded in DMSO. The proton NMR spectrum data of the histidine ligand indicates the appearance of a signal in the range of 12.89 ppm due to the presence $-\text{OH}$ carboxylic acid proton, this chemical shift of this proton is disappeared due to the involvement in the complexation toward selenium metal ions. In the aromatic region a few overlapping signals at range $9.00-6.10$ ppm, these signals are up field to lower chemical shift due to the involvement of nitrogen of pyridine ring in the complexation. The signal due to $-\text{NH}_2$ protons of histidine ligand appeared as a singlet peak at 8.64 ppm is shifted to up field (lower chemical shift) after coordination process due to sharing of nitrogen $-\text{NH}_2$ in chelation towards selenium metal ions. Another peak corresponding to protons of $-\text{NH}_2$ of nicotinamide is observed in the range of 7.80 ppm is not affected after complexation due to don't involvement in coordination.



Scheme 2. The association pathway of $[\text{Se}(\text{Nia})(\text{Trp})(\text{Cl})].2\text{Cl}$ complex.

$^1\text{H-NMR}$ (DMSO-d_6) spectral data of nicotinamide $\delta = 9.00, 8.76, 8.20, 7.55$ (4H, aromatic pyridine ring), and 7.80 (2H, NH_2); $^1\text{H-NMR}$ (DMSO-d_6) spectral data of tryptophan $\delta = 10.79$ (1H, NH indole ring), 12.89 (1H, $-\text{OH}$ propanoic acid), 8.71 (2H, NH_2), $7.58, 7.33, 7.20, 7.06, 6.98$ (5H, aromatic indole ring), 4.18 (1H, $-\text{CH}$ propanoic acid), and $3.31, 3.06$ (2H, $-\text{CH}_2$ propanoic acid); $^1\text{H-NMR}$ (DMSO-d_6) spectral data of $[\text{Se}(\text{Nia})(\text{Trp})(\text{Cl})].2\text{Cl}$ complex (Scheme 2) $\delta = 8.90, 8.60, 8.20, 7.80, 7.45, 6.92$ (protons of aromatic indole ring, pyridine ring and NH_2), $4.00, 2.45$ (protons of $-\text{CH}, -\text{CH}_2$ propanoic acid). The $^1\text{H NMR}$ spectrum of the $[\text{Se}(\text{Nia})(\text{Tph})(\text{Cl})].2\text{Cl}$ complex was recorded in DMSO. The proton NMR spectrum data of the tryptophan ligand indicates the appearance of a signal in the range of 12.89 ppm due to the presence $-\text{OH}$ carboxylic acid proton, this chemical shift of this proton is disappeared due to the involvement in the complexation toward selenium metal ions. In the aromatic region a few overlapping signals at range $8.90-6.92$ ppm, these signals are up field to lower chemical shift due to the nitrogen of nicotinamide-pyridine ring involvement in the complexation. The signal due to $-\text{NH}_2$ protons of tryptophan ligand appeared as a singlet peak at 8.71 ppm is shifted to up field (lower chemical shift) after coordination process due to sharing of nitrogen $-\text{NH}_2$ in chelation towards selenium metal ions. Another peak corresponding to protons of $-\text{NH}_2$ of nicotinamide is

observed in the range of 7.80 ppm is not affected after complexation due to don't involvement in coordination.



Scheme 3. The association pathway of [Se(Nia)(Tyr)(Cl)].2Cl complex.

¹H-NMR (DMSO-*d*₆) spectral data of nicotinamide $\delta = 9.00, 8.76, 8.20, 7.55$ (4H, aromatic pyridine ring), and 7.80 (2H, NH₂); ¹H-NMR (DMSO-*d*₆) spectral data of tyrosine $\delta = 9.06$ (1H, OH hydroxyphenyl ring), 12.89 (1H, -OH propanoic acid), 8.71 (2H, NH₂), 6.96, 6.68 (4H, aromatic hydroxyphenyl ring), 4.18 (1H, -CH propanoic acid), and 3.42, 3.17 (2H, -CH₂ propanoic acid); ¹H-NMR (DMSO-*d*₆) spectral data of [Se(Nia)(Tyr)(Cl)].2Cl complex (Scheme 3) $\delta = 8.60, 8.20, 7.75, 6.90, 6.80$ (protons of aromatic hydroxyphenyl ring, pyridine ring and NH₂), 3.60, 2.45 (protons of -CH, -CH₂ propanoic acid). The ¹H NMR spectrum of the [Se(Nia)(Tyr)(Cl)].2Cl complex was recorded in DMSO. The proton NMR spectrum data of the tyrosine ligand indicates the appearance of a signal in the range of 12.89 ppm due to the presence -OH carboxylic acid proton, this chemical shift of this proton is disappeared due to the involvement in the complexation toward selenium metal ions. In the aromatic region a few overlapping signals at range 8.60–6.80 ppm, these signals are up field to lower chemical shift due to the participation of nitrogen of nicotinamide-pyridine ring in the complexation. The signal due to -NH₂ protons of tyrosine ligand appeared as a singlet peak at 8.71 ppm is shifted to up field (lower chemical shift) after coordination process due to sharing of nitrogen -NH₂ in chelation towards selenium metal ions. Another peak corresponding to protons of -NH₂ of nicotinamide is observed in the range of 7.80 ppm is not affected after complexation due to don't involvement in coordination.

Nuclear magnetic resonance (NMR) spectroscopy confirmed the putative molecular structures of the metal complexes. Summarized, the peak at $\delta 8.71$ in the amino acid ligand due to proton of NH₂ shifted to up field in [Se(Nia)(His)(Cl)].2Cl, [Se(Nia)(Trp)(Cl)].2Cl and [Se(Nia)(Tyr)(Cl)].2Cl complexes because of coordination of the NH₂ group with selenium ion. Furthermore, another evidence of coordination at the site is that the δ (~9.00 – 6.00) of aromatic rings is slightly shifted. The absence of -OH of carboxylic group in the proton spectra of the three selenium metal complexes associated by mixed two ligands (nicotinamide and amino acids) substantiates the involvement of carboxylate-oxygen atom in the coordination mode.

Thermogravimetric analysis of the [Se(Nia)AA] complexes (I-3)

TGA curves of the three selenium(IV) complexes (I-III) showed the same thermal behavior. Thermal decomposition of complex (I) took place in three decomposition steps between 100–600 °C. The first step of decomposition occurred in the range 100–190 °C at maximum differential thermogravimetric peak DTG_{max} = 120 °C with mass loss 15% attributed to loss of Cl₂ molecule. The second step of decomposition occurred in the range 200–300 °C at maximum differential

thermogravimetric peak $DTG_{max} = 270$ °C with mass loss 67% attributed to loss of chloride ions and organic moieties include nicotinamide and histidine amino acid. The third decomposition step occurred at peak $DTG_{max} = 550$ °C with mass loss 16% attributed to loss of selenium by sublimation process. Few carbon atoms as residue after thermal cracking.

Thermogram of complex (II) has been shown in three decomposition stages. The first stage of decomposition occurs at maximum differential thermogravimetric peak $DTG_{max} = 110$ °C with mass loss 20% attributed to loss of 3Cl ions. The second stage of decomposition at $DTG_{max} = 265$ °C with mass loss 64% assigned to loss of nicotinamide, tryptophane organic molecules. The third stage occurred at peak $DTG_{max} = 580$ °C with mass loss 15% attributed to sublimation of selenium. few carbon atoms as residue after degradation.

The thermal decomposition of the complex (III) proceeds with two main degradations steps. The first stage occurs at a maximum temperature of 290 °C the found weight loss associated with this step is 82.7% and may be attributed to loss of 3Cl ions and two organic molecules tyrosine and nicotinamide which compatible with the calculated value of 82.4%. The second stage occurred at $DTG_{max} = 400$ °C with weight loss associated with this stage 17.6% which corresponding to sublimation of selenium.

Morphological analysis (XRD, SEM, TEM).

XRD spectrum of Se complex

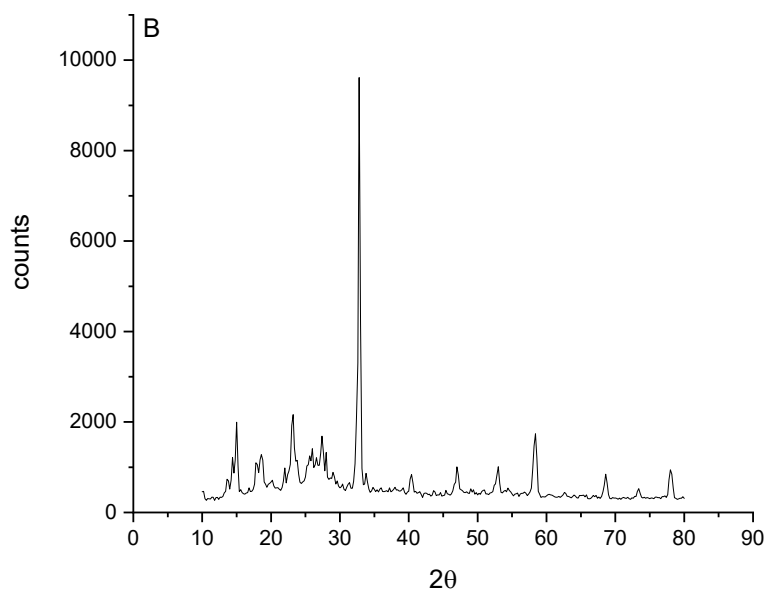
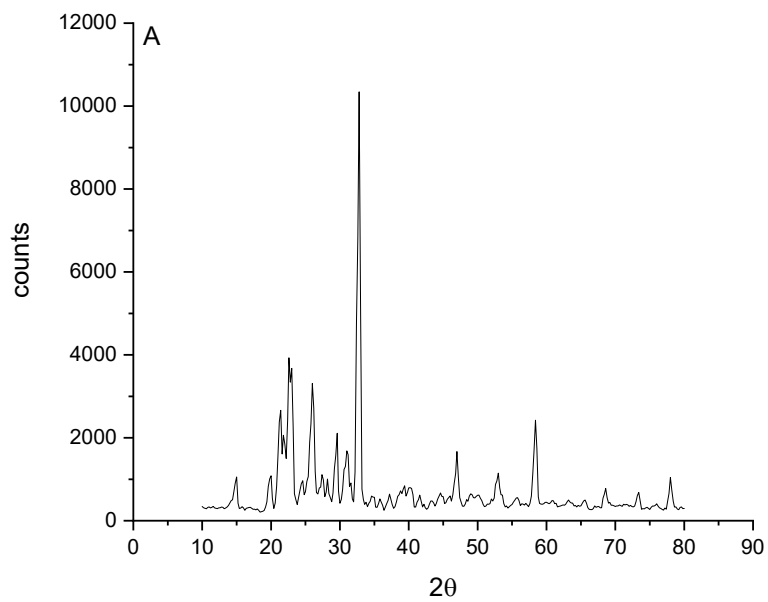
Figure 2 shows the X-ray diffraction patterns of Se complexes as SeNPs. The complex (I) shows the diffraction peaks located at 2θ are 14.8°, 19.8°, 21.2°, 22.8°, 25°, 26°, 27°, 28°, 29.5°, 31°, 32.7°, 46.9°, 52°, 58.3°, 68.3°, 73° and 77.9°, corresponding to the Se, Nia and His Planes of selenium complex. For complex (II) recorded diffraction peaks located at 2θ degree 14.87°, 18.66°, 21.8°, 23.2°, 25.8°, 27.4°, 29°, 32.8°, 47°, 52.8°, 58.3°, 68.5° and 78°, corresponding to the Se, Nia and Trp Planes of selenium complex. The diffractogram of complex (III) assigned diffraction peaks located at 2θ 22.6°, 23.2°, 32.7°, 40.4°, 46.9°, 52.9°, 58.3°, 68.5°, 58.3°, 72.3° and 77.9°, corresponding to the Se, Nia and Tyr Planes of selenium agreement with the data in literature [46]. The crystallite size of selenium was calculated using Scherrer's equation [47].

$$D = 0.89\lambda / \beta \cos \theta \quad (2)$$

where D = grain size, K = constant, taken to be 0.94, λ = wavelength of X-ray radiation, β is the full width at half maximum and θ is the angle of diffraction. The crystallite size was calculated and was found to be 5-10 nm for selenium nano particle.

SEM and TEM photos of Se(IV) complex

SEM images can also be seen that SeNPs are of several micrometers in length with diameters ranging from 5 μ m. The surface morphology was found to change with changes mixed ligand with images having large number of regularly shaped grains and small number of irregularly shaped grains. TEM images of Se(IV) complex nanoparticles resulting from the complex between Se(IV) chloride salt and two ligand (vitamin and amino acids) molecules are displayed in Figure 3. After chelation, the particle size was found to be within range of (5-10 nm) with spherical spots, which compatible with X-ray diffraction data.



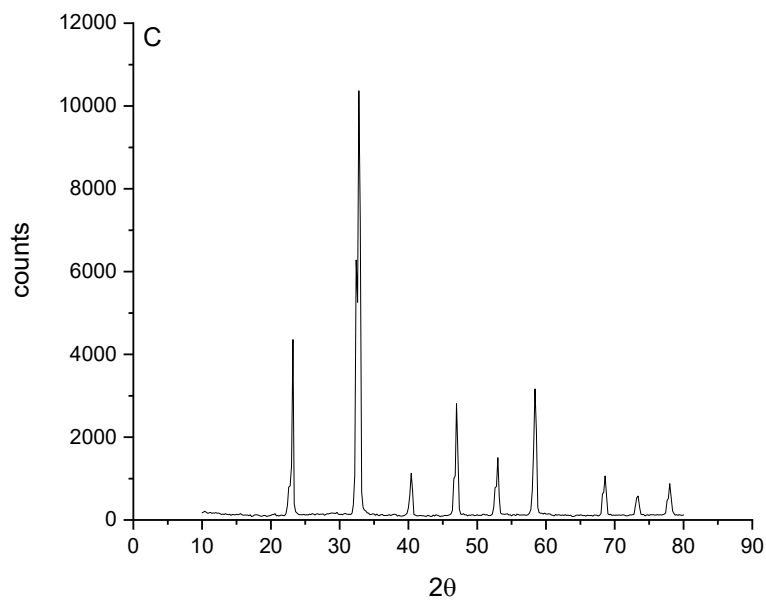


Figure 2. XRD spectrum of Se(IV) complexes (A) (Se/Nia/His), (B) (Se/Nia/Trp), and (C) (Se/Nia/Tyr).

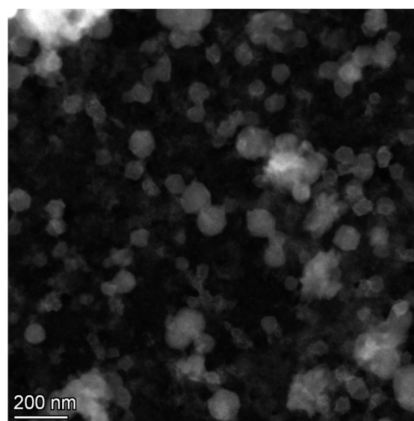


Figure 3A. TEM image of complex (Se/Nia/His).

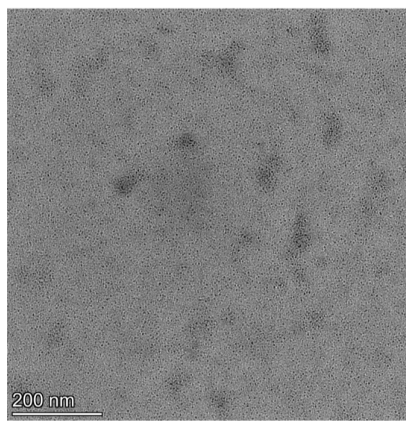


Figure 3B. TEM image of complex (Se/Nia/Trp).

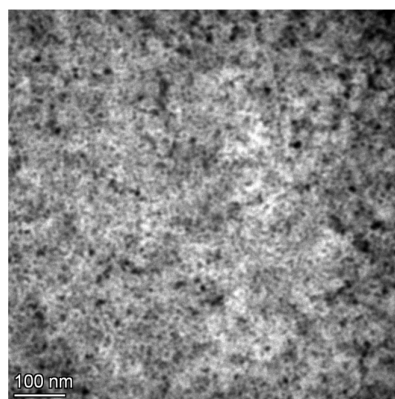


Figure 3C. TEM image of complex (Se/Nia/Tyr).

Antioxidant activity of Se complex

The antioxidant effect of synthesized selenium(IV) complexes (**1-3**) was evaluated using DPPH method. The chemical composition affects the radical scavenging activity of the tested compound (Table 3). At all concentrations (2.5, 5 and 10 $\mu\text{g/mL}$) the tested compounds (**1** and **2**) demonstrate moderate radical scavenging activity compared to ascorbic acid. The variation in the antioxidant effect results may be due to redox properties. Generally, chelate ring size, axial ligation degree of unsaturation in the chelate ring, are the factors which affect the redox properties of complexes [48].

Table 3. Antioxidant activity of compounds **1-3**.

Compound	% Inhibition			IC ₅₀ ($\mu\text{g/mL}$)
	at 2.5 $\mu\text{g/mL}$	at 5 $\mu\text{g/mL}$	at 10 $\mu\text{g/mL}$	
(Se/Nia/His)	24.73	28.17	32.09	30.46 \pm 0.37
(Se/Nia/Try)	17.48	20.39	25.87	23.74 \pm 0.31
(Se/Nia/Tyr)	10.67	17.28	25.09	21.29 \pm 0.25
Ascorbic acid	7.23	8.19	9.15	10.42 \pm 0.11

All experiments were carried out in triplicates and data are expressed as mean \pm SD.

Cytotoxicity effect of Se complex

The analysis (Table 4) revealed that compounds **1-3** has cytotoxic activity at the tested 50 μM concentration after 48 hours. The concentration that kills 50% of cells was determined after incubating the cells with serial dilutions (50, 25, 12.5, 6.25, 3.125, 1.56 μM) of each compound. Sorafenib was used as a positive control while 0.5% DMSO was used as a negative control. In vitro cytotoxicity activity of [Se(AA)(Nia)] complexes (**1-3**) were tested against HepG2, A2780 and HSF cell lines in the presence of sorafenib standard drug. The results evaluated upon determination of inhibitory concentration of (IC₅₀), the data was listed in Table 4. In comparison between data of Se (IV) complexes and sorafenib standard, the [Se(Tyr)(Nia)] complex has IC₅₀ equal 6.04 μM against HepG2 cell line and 6.98 μM against A2780. From these data can be deduced that [Se(Tyr)(Nia)] complex can be used as antitumor drug.

Table 4. IC₅₀ for compounds **1-3** towards the cancer cells. HSF = normal human skin fibroblast.

Compound	Cytotoxicity, IC ₅₀ (μM)		
	HepG2	A2780	HSF
(Se/Nia/His)	15.17 ± 0.64	7.92 ± 0.48	32.09 ± 0.65
(Se/Nia/Try)	11.92 ± 0.56	21.47 ± 1.03	24.81 ± 1.01
(Se/Nia/Tyr)	6.04 ± 0.33	6.98 ± 0.50	39.50 ± 0.79
Sorafenib	3.91 ± 0.23	7.50 ± 0.18	10.42 ± 0.51

All experiments were carried out in triplicates and data are expressed as mean ± SD.

ACKNOWLEDGEMENTS

This work was funded by the Deanship of Graduate Studies and Scientific Research at Jouf University under grant No. (DGSSR-2023-02-02264).

REFERENCES

- Odom, J.D.; Dawson, W.H.; Ellis, P.D. Selenium-77 relaxation time studies on compounds of biological importance: Dialkyl selenides, dialkyl diselenides, selenols, selenonium compounds, and seleno oxyacids. *J. Am. Chem. Soc.* **1979**, *101*, 5815–5822.
- Xu, H. *Selenium: Its Chemistry, Biochemistry and Application in Life Science (in Chinese)*, Huazhong University: China; **1994**.
- Robberecht, H.J.; Deelstra, H.A. Selenium in human urine determination, speciation and concentration levels. *Talanta* **1984**, *31*, 497–508.
- Barceloux, D.G.; Barceloux, D. Selenium. *J. Toxicol. Clin. Toxicol.* **1999**, *37*, 145–172.
- Rotruck, J.T.; Pope, A.L.; Ganther, H.E.; Swanson, A.B.; Hafeman, D.G.; Hoekstra, W. Selenium: biochemical role as a component of glutathione peroxidase. *Science* **1973**, *179*, 588–590.
- Kobayashi, Y.; Ogra, Y.; Ishiwata, K.; Takayama, H.; Aimi, N.; Suzuki, K.T. Selenosugars are key and urinary metabolites for selenium excretion within the required to low-toxic range. *Proc. Natl. Acad. Sci. USA* **2002**, *99*, 15932–15936.
- Combs, G.F. Selenium in global food systems. *Br. J. Nutr.* **2001**, *85*, 517–547.
- Finley, J.W.; Penland, J.G. Adequacy or deprivation of dietary selenium in healthy men: Clinical and psychological findings. *J. Trace. Elem. Exp. Med.* **1998**, *11*, 11–27.
- Tamas, L. A Szelen Betegsegmegelozo szerepe. *Komplementer Med.* **2000**, *4*, 16–20.
- Reilly, C. Selenium: a new entrant into the functional food arena. *Trends Food Sci. Technol.* **1998**, *9*, 114–118.
- Bankhofer, H. Bio-Selen: Natürlicher Schutz für unser Abwehrsystem, Herbig; **1988**.
- Burk, R.F.; Lane, J.M. Modification of chemical toxicity by selenium deficiency. *Toxicol. Sci.* **1983**, *3*, 218–221.
- Urdaneta, N.; Madden, W.; Landaeta, V.R.; Rodríguez-Lugo, R.; Hernández, L.; Lubes V. Formation studies of binary and ternary complexes of copper(II) with an oxazol derivative of nicotinic acid and some amino acids. *J. Mol. Liq.* **2017**, *217*, 218–222.
- Roman, L.; Bârzu, O.; Implicații biomedicale ale combinațiilor complexe. *Editura Dacia* **1979**, *82*, 1–230.
- Kaback, H.R. A molecular mechanism for energy coupling in a membrane transport protein, the lactose permease of *Escherichia coli*. *Proc. Natl. Acad. Sci. USA* **1997**, *94*, 5539–5543.
- Power, R.; Horgan, K. *Biological Chemistry and Absorption of Inorganic and Organic Trace Metals*. In: Lyons, T.P.; Jacques, K.A. (Eds.), 1st ed., Nottingham University Press: Nottingham, UK; **2000**; pp. 277–291.

17. Newsholme, P.; Stenson L.; Sulvucci, M.; Sumayao, R.; Krause, M. *Amino Acid Metabolism*, in *Comprehensive Biotechnology*, Elsevier: Amsterdam; **2011**, pp. 3–14.
18. Asemave, K.; Yiase, S.G.; Adejo, S.O.; Anhwange, B.A. Kinetics and mechanism of substitution reaction of trans-dichlorobis (ethylenediammine) cobalt(III) chloride with aspartic acid. *Int. J. Inorg. Bioinorg. Chem.* **2011**, 2, 11–14.
19. Boruah, D. Interaction of cobalt(II) and nickel(II) ions with Amino acids in aqueous solution: A spectrophotometric study. *Int. J. Sci. Res. Pub.* **2012**, 2, 1–4.
20. Dinelli, L.R.; Bezerra, T.M.; Sene, J.J. A kinetic study of the reaction between trans-[CoCl₂(en)₂]Cl and the amino-acids alanine and valine. *Curr. Res. Chem.* **2010**, 2, 18–23.
21. Norbert, S.; JaKubke, H.D. *Peptides, Chemistry and Biology*, Wiley: New York; **2002**; pp. 3–590.
22. Greenstein, J.P.; Winitz, M. *Chemistry of the Amino Acids*, John Wiley & Sons: New York; **1961**; p. 763.
23. Sun, L.; Burkitt, M.; Tamm, M.; Raymond, M.K.; Abrahamsson, M.; LeGourriérec, D.; Frapart, Y.; Magnuson, A.; Kenez, P.H.; Brandt, P. Hydrogen-bond promoted intramolecular electron transfer to photogenerated Ru(III): A functional mimic of tyrosine and histidine 190 in Photosystem II. *J. Am. Chem. Soc.* **1999**, 121, 6834–6842.
24. Kiss, T.; Gergely, A. Complex-forming properties of tyrosine isomers with transition metal ions. *J. Chem. Soc. Dalton Trans.* **1984**, 1951–1957.
25. Letter Jr, J.E.; Bauman Jr, J.E. Thermodynamic study of the complexation and coordinated ligand deprotonation reactions for a series of tyrosine isomers with copper(II). *J. Am. Chem. Soc.* **1970**, 92, 443–447.
26. Qu, Q.; Hao, Z.; Jiang, S.; Li, L.; Bai, W. Synergistic inhibition between dodecylamine and potassium iodide on the corrosion of cold rolled steel in 0.1 M phosphoric acid. *Mater. Corros.* **2008**, 59, 883–888.
27. Anastasi, G.; Antonelli, M.L.; Biondi, A.; Vinci, G. Orotic acid: A milk constituent: Enzymatic determination by means of a new microcalorimetric method. *Talanta* **2000**, 52, 947–952.
28. Bratu, I.; Gavira-Vallejo, J.M.; Hernanz, A.; Bogdan, M.; Bora, G. Inclusion complex of fenbufen with β -cyclodextrin. *Biopolym. Original Res. Biomol.* **2004**, 73, 451–456.
29. Bratu, I.; Gavira-Vallejo, J.M.; Hernanz, A. ¹H-NMR study of the inclusion processes for α - and γ -cyclodextrin with fenbufen. *Biopolym. Original Res. Biomol.* **2005**, 77, 361–367.
30. Bratu, I.; Veiga, F.; Fernandes, C.; Hernanz, A.; Gavira, J.M. Infrared spectroscopic study of triacetyl- β -cyclodextrin and its inclusion complex with nicardipine. *Spectroscopy* **2004**, 18, 459–467.
31. Immel, S.; Schmitt, G.E.; Lichtenthaler, F.W. *α -Cycloaltrin: Conformation and Properties in the Solid-State and Aqueous Solution [I]* in *Proceedings of the Ninth International Symposium on Cyclodextrins: Santiago de Compostela, Spain*, **1998**, 3, 41–48.
32. Coulson, R.A.; Hernandez, T. Alligator metabolism studies on chemical reactions in vivo. *Comp. Biochem. Physiol. B* **1983**, 74, 1-182
33. Lieberman, I.; Kornberg, A.; Simms, E.S. Enzymatic synthesis of pyrimidine nucleotides. Orotidine-5'-phosphate and uridine-5'-phosphate. *J. Biol. Chem.* **1955**, 215, 403–415.
34. Arrizabalaga, P.; Castan, P.; Dahan, F. Coordination sites of 5-nitro-6-carboxyuracil: UV study and X-ray structure determination of diammine (5-nitroorotato) copper(II) hydrate and hexaamminebis (5-nitroorotato) tricopper(II) pentahydrate. *Inorg. Chem.* **1983**, 22, 2245–2252.
35. Bach, I.; Kumberger, O.; Schmidbaur, H. Orotate complexes. Synthesis and crystal structure of lithium orotate (—I) monohydrate and magnesium bis [orotate (—I)] octahydrate. *Chem. Ber.* **1990**, 123, 2267–2271.
36. Psoda, A.; Kazimierzczuk, Z.; Shugar, D. Structure and tautomerism of the neutral and monoanionic forms of 4-thiouracil derivatives. *J. Am. Chem. Soc.* **1974**, 96, 6832–6839.

37. Althagafi, I.I.; Gaffer, H.E. Synthesis, molecular modeling and antioxidant activity of new phenolic bis-azobenzene derivatives. *J. Mol. Struct.* **2019**, *1182*, 22–30.
38. Mosmann, T. Rapid colorimetric assay for cellular growth and survival: application to proliferation and cytotoxicity assays. *J. Immunol. Methods* **1983**, *65*, 55–63.
39. El-Senduny, F.F.; Shabana, S.M.; Rösel, D.; Brabek, J.; Althagafi, I.; Angeloni, G.; Manolikakes, G.; Shaaban, S. Urea-functionalized organoselenium compounds as promising anti-HepG2 and apoptosis-inducing agents. *Future Med. Chem.* **2021**, *13*, 1655–1677.
40. Elimam, D.M.; Elgazar, A.A.; El-Senduny, F.F.; El-Domany, R.A.; Badria, F.A.; Eldehna, W.M. Natural inspired piperine-based ureas and amides as novel antitumor agents towards breast cancer. *J. Enzyme Inhib. Med. Chem.* **2022**, *37*, 39–50.
41. Gad, E.A.M.; Al-Fahemi, J.H. Adsorptivity and corrosion inhibition performance of 2-(alkyloxy)-N,N,N-tris (2-hydroxyethyl)-2-oxoethanaminium chloride using DFT approach. *Int. J. Sci. Eng. Res.* **2015**, *6*, 570–576.
42. Frisch, M.J.; Trucks, G.W.; Schlegel, H.B.; Scuseria, G.E.; Robb, M.A.; Cheeseman, J.R.; Montgomery, Jr. J.A.; Vreven, T.; Kudin, K.N.; Burant, J.C.; Millam, J.M.; Iyengar, S.S.; Tomasi, J.; Barone, V.; Mennucci, B.; Cossi, M.; Scalmani, G.; Rega, N.; Petersson, G.A.; Nakatsuji, H.; Hada, M.; Ehara, M.; Toyota, K.; Fukuda, R.; Hasegawa, J.; Ishida, M.; Nakajima, T.; Honda, Y.; Kitao, O.; Nakai, H.; Klene, M.; Li, X.; Knox, J.E.; Hratchian, H.P.; Cross, J.B.; Bakken, V.; Adamo, C.; Jaramillo, J.; Gomperts, R.; Stratmann, R.E.; Yazyev, O.; Austin, A.J.; Cammi, R.; Pomelli, C.; Ochterski, J.W.; Ayala, P.Y.; Morokuma, K.; Voth, G.A.; Salvador, P.; Dannenberg, J.J.; Zakrzewski, V.G.; Dapprich, S.; Daniels, A.D.; Strain, M.C.; Farkas, O.; Malick, D.K.; Rabuck, A.D.; Raghavachari, K.; Foresman, J.B.; Ortiz, J. V.; Cui, Q.; Baboul, A.G.; Clifford, S.; Cioslowski, J.; Stefanov, B.B.; Liu, G.; Liashenko, A.; Piskorz, P.; Komaromi, I.; Martin, R.L.; Fox, D.J.; Keith, T.; Al-Laham, M.A.; Peng, C.Y.; Nanayakkara, A.; Challacombe, M.; Gill, P.M.W.; Johnson, B.; Chen, W.; Wong, M.W.; Gonzalez, C.; Pople, J.A. *Gaussian 03, Revision E.01*, Gaussian: USA; **2004**.
43. El-Habeeb, A.A.; Refat, M.S. Synthesis, structure interpretation, antimicrobial and anticancer studies of tranexamic acid complexes towards Ga(III), W(VI), Y(III) and Si(IV) metal ions. *J. Mol. Struct.* **2019**, *1175*, 65–72.
44. Cotton F. A., Holm, R.H. Nuclear magnetic resonance and ultraviolet spectra of acetylacetonates. *J. Amer. Chem. Soc.* **1958**, *80*, 5658–5663.
45. Demir, S.; Yilmaz, V.T.; Sariboga, B.; Buyukgungor, O.; Mrozinski, J. Metal(II) nicotinamide complexes containing succinato, succinate and succinic acid: Synthesis, crystal structures, magnetic, thermal, antimicrobial and fluorescent properties. *J. Inorg. Organomet. Polym. Mater.* **2010**, *20*, 220–228.
46. Saad, F.A.; El-Metwaly, N.M.; Refat, M.S.; Khedr, A.M. Synthesis and characterization of new nano-sized selenium compounds to further use as antioxidants drugs. *Russ. J. Gen. Chem.* **2018**, *88*, 1258–1265.
47. Cullity, B.D. Elements of X-ray diffraction, **1978**, 103, 292.
48. Raja, D.S.; Bhuvanesh, N.S.P.; Natarajan, K. A novel water-soluble ligand bridged cobalt(II) coordination polymer of 2-oxo-1,2-dihydroquinoline-3-carbaldehyde (isonicotinic) hydrazone: evaluation of the DNA binding, protein interaction, radical scavenging and anticancer activity. *Dalton Trans.* **2012**, *41*, 4365–4377.